Parametric Study to Evaluate the Effect of Strut Geometry on PLLA Coronary Stent Recoil

R. Blair[1], N. Dunne[2-4], A. Lennon[1] and G. Menary[1]

1 School of Mechanical and Aerospace Engineering, Queen's University, Belfast, UK

2 Centre for Medical Device Engineering, School of Mechanical and Manufacturing Engineering, Dublin City University, Ireland

3 School of Pharmacy, Queen's University, Belfast, UK

4 Trinity Centre for Bioengineering, Trinity College Dublin, Ireland

email: (rblair522@qub.ac.uk)

Abstract*: Bioresorbable poly(L-lactic acid) (PLLA) stents present a clinically attractive treatment for coronary heart disease, providing a temporary scaffold that resorbs once the artery has healed. Polymeric stents are often mechanically inferior to their permanent metallic counterparts. However, their mechanical properties can be tailored through stretch-blow molding (SBM); a process that induces crystallinity and molecular orientation, subsequently altering the mechanical response of the polymer. This study aims to quantify the variation in mechanical properties of PLLA as a result of the SBM procedure and investigate the functionality of a stent constructed from this polymer. A custom-built biaxial stretching machine was used to replicate the SBM process and a rate-independent plasticity constitutive model was calibrated using uniaxial test data of specimens punched from biaxially stretched sheet. Stent expansion simulation procedures were performed on idealized geometry using an explicit solution procedure within Abaqus v6.14. A parametric study was conducted to assess the impact of strut width and strut length on stent recoil, from a cohort of eleven unique scaffold geometries. Results of the study show that a PLLA scaffold is required to have large values of strut width combined with short circumferential rings in order to significantly reduce recoil and contend with the performance of a metallic stent.*

Keywords*: Stent, Biomechanics, Polymer, Poly(L-lactic acid), PLLA, Constitutive Model, Plasticity, Parametric Study.*

1. Introduction

Coronary heart disease (CHD) is the largest cause of death in the United Kingdom each year and is commonly caused by atherosclerosis, an inflammatory disease that hardens and narrows the artery (Ludman et al., 2016). Coronary stents are small expandable scaffolds deployed at the site of an atherosclerotic lesion in order to dilate the artery and restore patency. Typically, coronary stents are manufactured from high strength metallic alloys such as stainless steel (316L) and cobalt-chromium L605 (CoCr) (Grogan et al., 2012), however these scaffolds remain in the body-post procedure and have the potential to trigger an undesirable immunological response (Bourantas et al., 2013). Bioresorbable polymer stents offer a potentially clinically attractive solution, providing a temporary scaffold that resorbs once the artery has healed.

Poly(L-lactic acid) (PLLA) has been used as a successful platform material of a bioresorbable stent with the Absorb Bioresorbable Vascular Scaffold (BVS) gaining U.S. Food and Drug Administration approval in July, 2016 (U.S. Food and Drug Administration, 2016). A key benefit is the ability to control mechanical properties through tailoring chemical composition and processing history. Stretch-blow molding (SBM) has been shown to increase crystallinity content and orientate PLLA (Løvdal et al., 2015), which subsequently influences the mechanical response (Bergström and Hayman, 2015). Hence, it is important that the processing history of the polymer is accounted for when developing a constitutive model for finite element simulations.

The use of finite element analysis (FEA) is especially prevalent within the discipline of computational biomechanics, where *in vivo* testing and validation is exceptionally difficult. Finite element analysis presents an invaluable tool for preclinical simulation of modern procedures, whereby the efficacy of a stent may be evaluated and its geometry optimized prior to any form of physical testing.

Within this study, the impact of strut geometry on the measured recoil of a given PLLA scaffold design was investigated. A constitutive material model for PLLA was calibrated against uniaxial test data and a parametric study was performed in order to evaluate the effect of strut width and strut length on stent recoil, from a cohort of eleven unique scaffold geometries. Stent recoil was measured for each scaffold geometry and compared to that of a stainless steel 316L stent. Details of material testing, constitutive models, simulation procedures and stent geometries are discussed in subsequent sections.

2. Material Testing

Poly(L-lactic acid) pellets (approximately 5 % D-isomer) were obtained from Corbion Purac (Amsterdam, The Netherlands) and extruded into 0.5 mm thick sheet. A custom-built biaxial tensile test machine (Queen's University Belfast, Northern Ireland) was used to replicate the processing history induced during the SBM process. The material was heated above its glass transition temperature of 63 °C , determined using differential scanning calorimetry (DSC), and biaxially stretched to two stretch ratios (λ = 2 and 2.5) at two strain rates ($\dot{\varepsilon}$ = 1 s^{-1} and 4 s^{-1}). Inducing stress in the polymer at a temperature 10 °C above the glass transition temperature, followed by a heat-setting period, has been shown to permit orientation and promote the development of a crystalline structure (Lunt, 1998). For this reason, a processing temperature of 75 °C was held constant throughout.

Uniaxial tensile testing in accordance with ISO 527 was performed using dumb-bell specimens (n = 5) of PLLA in the machine (extrusion) direction under ambient laboratory conditions (20 °C) at an extension rate similar to that recommended for bioresorbable scaffold deployment (2.5 mm/min), according to published guidelines from Abbott (Abbott Vascular, Santa Clara, USA). Specimens punched from un-stretched sheet were compared to those punched from biaxially stretched sheet. A visible increase in yield strength as a function of the stretch ratio during processing was observed (Figure 1), with a maximum increase on average of 28 % during processing at a stretch ratio of λ = 2.5 and a strain rate of $\dot{\varepsilon}$ = 1 s^{-1}. It is expected that the increase in yield stress is as a result of strain induced crystallization and molecular orientation induced during the biaxial stretching procedure (Lovdal et al., 2015).

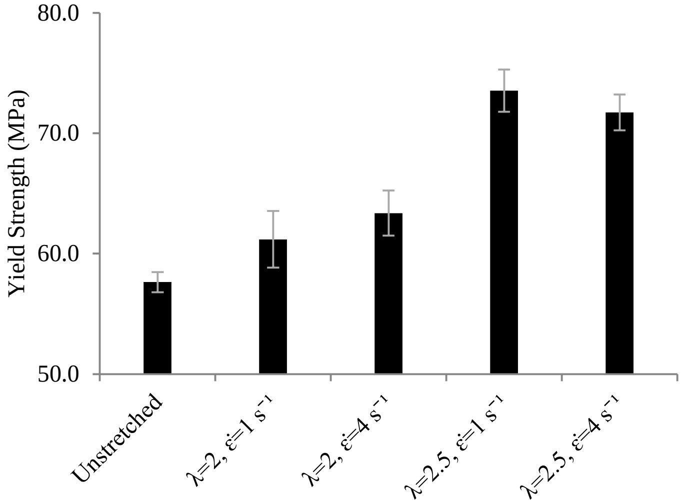

Figure 1. Increase in yield strength due to the biaxial stretching process.

Elongation to break was significantly increased post-biaxial stretching. According to Witzke (1997), the molecular orientation induced during SBM reduces the effect of aging through stabilization of the polymer free volume, with crystallites formed as a result of the SBM process also acting as physical crosslinks to stabilize the amorphous domain, reducing the polymer's brittleness (Lim et al., 2008). The constitutive model developed in the subsequent section was calibrated against post-biaxial stretched (λ = 2.5 and $\dot{\varepsilon}$ = 1 s^{-1}) samples, given the enhanced mechanical properties observed upon testing.

3. Constitutive Modeling

A rate-independent isotropic piece-wise hardening plasticity model was employed in order to capture the material response of PLLA, through the application of finite deformation continuum mechanics. The constitutive model presented is available as a built-in material model within Abaqus. A rate-independent material model was generated for the stainless steel 316L based on the data published by Murphy et al. (2003). In this study, the stress-strain behavior of coronary stent struts was shown to be dependent on the size, especially when considering strut thicknesses that approach the grain size of the material. The material data for PLLA and stainless steel 316L is shown in Figure 2, from which both of the respective material models are calibrated.

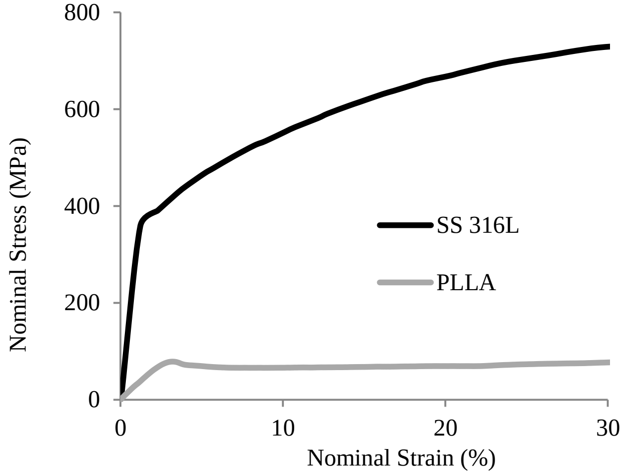

Figure 2. Material data for constitutive model calibration.

4. Simulation Procedure

An idealized quasi-static expansion procedure was simulated in Abaqus/Explicit v6.14 (Dassault Systèmes, Providence, RI, USA) using a displacement driven cylinder (meshed with S4R shell elements) and a deformable solid stent (meshed with C3D8R brick elements), as shown in Figure 3. A unit cell was used to represent the full length stent geometry in order to reduce computational cost and was constrained in both the axial and tangential directions (with respect to a user-defined cylindrical coordinate system) via three nodes forming an equilateral triangle in the central section. A radial displacement was prescribed to all nodes on the cylinder increasing its diameter from 1.0 mm to 3.5 mm using the smooth-step amplitude definition within Abaqus, with tangential and axial displacement prohibited.

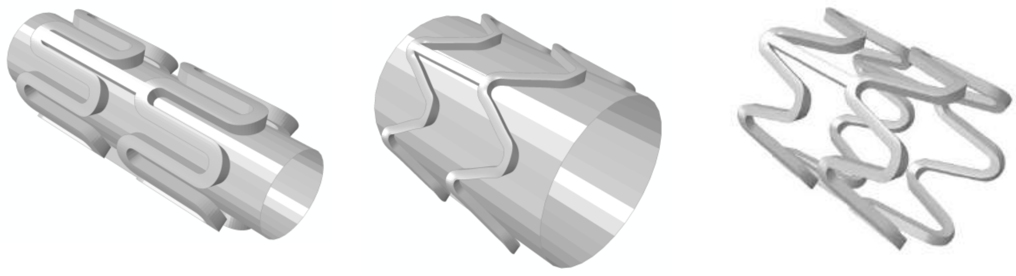

(a) Initial (b) Inflation (c) Recoil

Figure 3. Simulation procedures.

The time-frame typically required for polymeric stent expansion approaches one minute; according to published guidelines from Abbott (Abbott Vascular, Santa Clara, USA). However, given that a rate-independent material model is used, the time frame for expansion was accelerated using an explicit solution procedure with a time step of 0.05 s; this is comparable to time step values found in published literature (Bukala et al., 2015; Schiavone et al., 2015), with smaller time increments yielding excessively high loading rates and significant inertial effects. In general, for a quasi-static simulation procedure, the impact velocity should be maintained at less than 1 % of the wave speed in the material and the kinetic energy of the deforming material should not exceed 5 % of its internal energy throughout the majority of the analysis (Dassault Systèmes, 2014). Figure 4 shows an energy plot highlighting the total internal energy (IE) and total kinetic energy (KE) throughout the simulation.

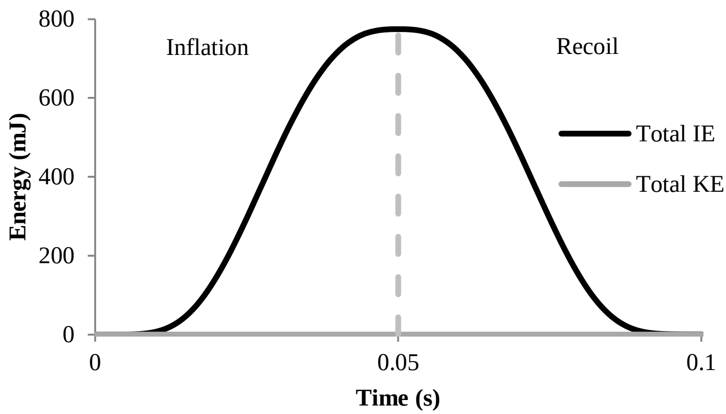

Figure 4. Energy plot for the quasi-static simulation procedure.

Mass-proportional damping was employed to mitigate spurious oscillations, with the damping constant, α_R, (Equation 1) selected to provide a damping ratio of 0.1 (10 %), based on the lowest natural frequency of the crimped stent structure (for both PLLA and stainless steel 316L variants) obtained through a free (unconstrained) modal analysis.

$$\zeta_i = \frac{\alpha_R}{2\omega_i} \tag{1}$$

where ζ_i and ω_i denote the damping ratio and natural frequency respectively for a given mode, i, and α_R denotes the damping constant.

5. Methodology

The scaffold geometry used in the present study was based on the refined stent design from a parametric optimization study on metallic scaffolds by Bedoya et al. (2006) and resembles the geometry of the commercially available Multilink stent (Advanced Cardiovascular Systems, Santa Clara, USA). Six parametric stent geometries were generated by varying the strut width, W_{strut}, evenly within the range of 100 μm to 150 μm, holding the strut length, L_{strut}, constant at 1000 μm (Figure 5). An additional five stent geometries were generated by varying the strut length evenly between the range of 500 μm and 900 μm, holding the strut width constant at 150 μm. Strut width and the axial length of a circumferential ring have both been shown to have a significant effect on the mechanical performance of a stent (Migliavacca et al., 2002; Pant et al., 2011).

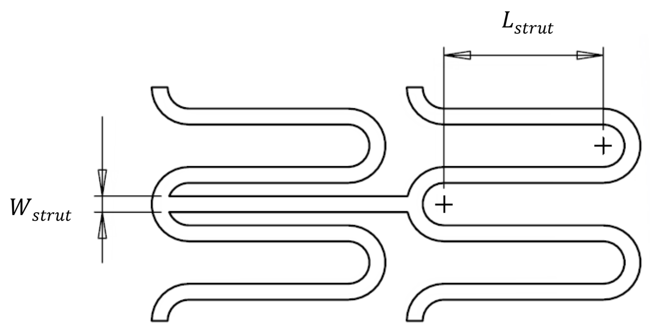

Figure 5. Geometry parameterization.

Stent recoil was calculated using Equation 2 and expressed as a percentage:

$$Recoil = \frac{D_{initial} - D_{final}}{D_{initial}} \tag{2}$$

where $D_{initial}$ denotes the internal stent diameter at the end of the inflation step and D_{final} denotes the internal stent diameter post-recoil.

6. Results

Figure 6 shows the effect of strut width on recoil for both PLLA and stainless steel 316L stent designs, holding the strut length constant at 1000 μm. Increasing strut width from 100 μm to 150 μm reduced recoil from 54 % to 37 % for a PLLA scaffold and reduced recoil from 5.6 % to 4.3 % for a stainless steel 316L scaffold. The measured recoil of approximately 5 % for the stainless steel stent design is comparable to that of a typical open cell metallic stent design, based on published literature (Grogan et al., 2012; Lanzer, 2007). Figure 7 shows the effect of strut length on recoil for PLLA, holding the strut width constant at 150 μm. Decreasing strut length from 1000 μm to 500 μm further reduced recoil from 37 % to 14 % for a PLLA scaffold.

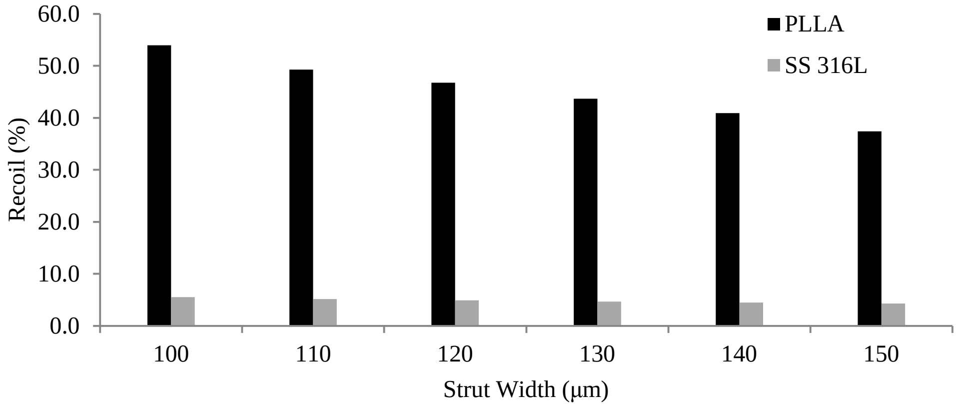

Figure 6. Effect of strut width on stent recoil for PLLA and stainless steel 316L (SS 316L).

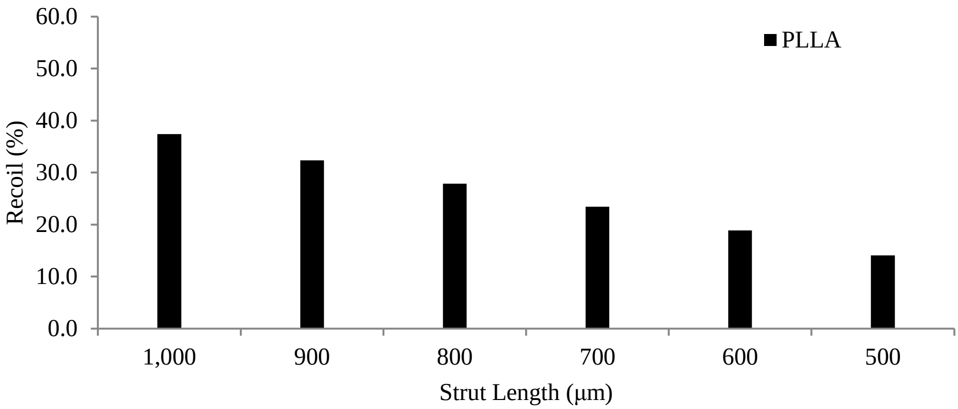

Figure 7. Effect of strut length on stent recoil for PLLA.

Maximum plastic strains were observed at strut hoops, which act as mechanical hinges during deformation (Figure 8). The increased levels of recoil for the polymer (PLLA) scaffolds are primarily due to a lack of plastic strain in these regions. In general, the plastic strain did not progress through the width of a PLLA strut hoop, leaving a region of elasticity that caused a springback effect, resulting in higher levels of recoil. When compared to a scaffold constructed from stainless steel 316L with similar strut width, plastic straining through the width was observed. Decreasing strut length further reduced recoil through increased plastic straining in the strut hoops (Figure 9).

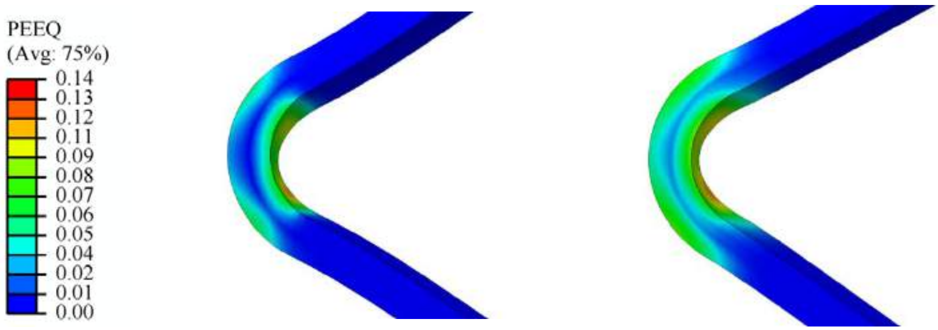

(a) PLLA (b) Stainless steel 316L

Figure 8. Equivalent plastic strain (PEEQ) at maximum deformation for a strut width of 120 µm and a strut length of 1000 µm.

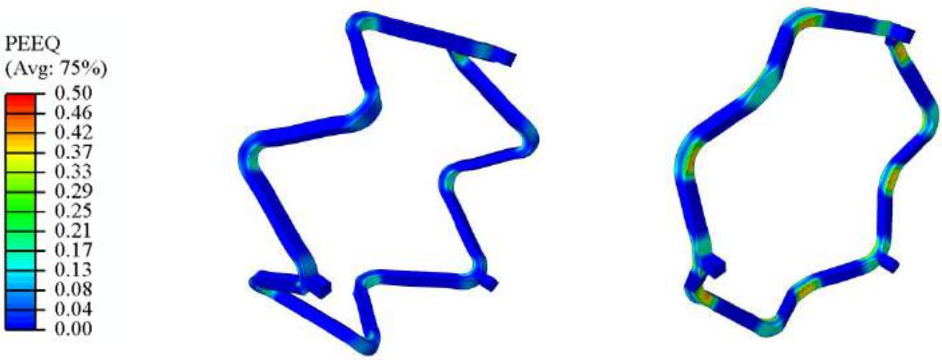

(a) Strut length of 1000 µm (b) Strut length of 500 µm

Figure 9. Equivalent plastic strain (PEEQ) at maximum deformation for a PLLA strut width of 150 µm.

7. Discussion

The baseline scaffold geometry presented is intended for a metallic (e.g. stainless steel 316L) based stent and is not ideally suited to PLLA, as it does not induce high levels of plastic deformation throughout the strut width, resulting in excessive recoil. It is hypothesized that a geometry intended for metallic scaffolds is not always transferable to polymeric scaffolds, with parametric optimization simply refining a non-optimal strut shape. Suitable baseline scaffold geometry should first be identified prior to parametric optimization through the use of a topology based optimization procedure, suggesting a use for the Tosca module available within Abaqus.

8. Conclusion

A parametric study was conducted to assess the impact of strut width and strut length on stent recoil, from a cohort of eleven unique scaffold geometries. Results of the study show that a PLLA scaffold is required to have large values of strut width combined with short circumferential rings in order to significantly reduce recoil and contend with the performance of a metallic stent.

To the best of the authors' knowledge, no published study has sought to perform a parametric study on PLLA scaffolds that accounts for the stretch-blow molding processing history, presenting a novel area of research. It is hypothesized that the parametric study outlined herein may be used as a tool to influence stent geometry selection during the early stages of the design process.

9. Future Work

A preliminary framework has been developed that permits the parametric analysis and performance assessment of a given stent geometry. The framework does however suffer from some limitations and areas for potential improvement.

In order to perform a comprehensive evaluation of scaffold performance, additional design parameters must be considered, such as strut thickness, strut spacing and number of struts per circumferential ring. Further simulations should also be developed to evaluate a number of other performance metrics on the expanded scaffold, taken from published literature (Bobel et al., 2015; Pauck and Reddy, 2015; Grogan et al., 2012, Pant et al., 2011; Li et al., 2017), namely radial strength, flexibility and longitudinal resistance.

A rate-independent plasticity material model was used for PLLA. Literature has shown PLLA to exhibit rate-dependent anisotropic viscoplastic behavior (Eswaran et al., 2011) and hence, a more complex material model capable of capturing these nonlinearities will be required for future studies. It is intended that the Parallel Rheological Framework (PRF) model (available as a built-in model within Abaqus) will be used in conjunction with Isight for the calibration procedure.

The impact of the stent on the artery was neglected during the parametric study. Neglecting the artery permits a parametric analysis to return a mechanically superior design that is not compatible with an artery, e.g. excessively thick struts that may promote restenosis. Consequently, inclusion of an artery model will be necessary in future studies.

10. References

1. Abbott Vascular. Absorb GT1™ Bioresorbable Vascular Scaffold (BVS) System Instructions for Use, Santa Clara, California, USA, 2016.
2. Bedoya, J., Meyer, C.A., Timmins, L.H., Moreno, M.R. And Moore, J.E., 2006. Effects of Stent Design Parameters on Normal Artery Wall Mechanics. Journal of Biomechanical Engineering, 128(5), pp. 757-765.
3. Bergström, J.S. and Hayman, D., 2015. An Overview of Mechanical Properties and Material Modeling of Polylactide (PLA) for Medical Applications. Annals of Biomedical Engineering, pp. 1-11.
4. Bobel, A., Petisco, S., Sarasua, J.R., Wang, W. and Mchugh, P., 2015. Computational Bench Testing to Evaluate the Short-Term Mechanical Performance of a Polymeric Stent. Cardiovascular Engineering and Technology, 6(4), pp. 519-532.
5. Bourantas, C.V., Onuma, Y., Farooq, V., Zhang, Y., Garcia-Garcia, H.M. and Serruys, P.W., 2013. Bioresorbable Scaffolds: Current Knowledge, Potentialities and Limitations Experienced During their First Clinical Applications. International Journal of Cardiology, 167(1), pp. 11-21.
6. Bukala, J., Kwiatkowski, P. and Malachowski, J., 2015. Numerical Analysis of Stent Expansion Process in Coronary Artery Stenosis with the use of Non-Compliant Balloon. Biocybernetics and Biomedical Engineering. Biocybernetics and Biomedical Engineering, 36(1), pp. 145-156.
7. Dassault Systemès. Abaqus Version 6.14, Analysis User's Manual. Providence, RI, 2014.
8. Eswaran, S.K., Kelley, J.A., Bergstrom, J.S. and Giddings, V.L., 2011. Material modeling of polylactide, SIMULIA Customer Conference 2011, pp. 1-11.
9. Grogan, J.A., Leen, S.B. and Mchugh, P.E., 2012. Comparing Coronary Stent Material Performance on a Common Geometric Platform through Simulated Bench Testing. Journal of the Mechanical Behavior of Biomedical Materials, 12, pp. 129-138.
10. Lanzer, P., Mastering Endovascular Techniques: A Guide to Excellence. Lippincott Williams & Wilkins, 2007.
11. Li, H., Wang, X., Wei, Y., Liu, T., Gu, J., Li, Z., Wang, M., Zhao, D., Qiao, A. and Liu, Y., 2017. Multi-Objective Optimizations of Biodegradable Polymer Stent Structure and Stent Microinjection Molding Process. Polymers, 9(1), pp. 20.
12. Lim, L., Auras, R. and Rubino, M., 2008. Processing Technologies for Poly (Lactic Acid). Progress in Polymer Science, 33(8), pp. 820-852.
13. Løvdal, A., Andreasen, J.W., Mikkelsen, L.P., Agersted, K. and Almdal, K., 2016. Characterization of Biaxial Strain of Poly (L-Lactide) Tubes. Polymer International, 65(1), pp. 133-141.
14. Ludman, P. (et al.), National Audit of Percutaneous Coronary Interventions Annual Public Report, British Cardiovascular Intervention Society, 2016.
15. Lunt, J., 1998. Large-Scale Production, Properties and Commercial Applications of Polylactic Acid Polymers. Polymer Degradation and Stability, 59(1), pp. 145-152.

16. Migliavacca, F., Petrini, L., Colombo, M., Auricchio, F. and Pietrabissa, R., 2002. Mechanical Behavior of Coronary Stents Investigated Through the Finite Element Method. Journal of Biomechanics, 35(6), pp. 803-811.

17. Murphy, B. P., Savage, P., McHugh, P. E. and Quinn, D. F., 2003. The Stress–Strain Behavior of Coronary Stent Struts is Size Dependent. Annals of Biomedical Engineering, 31(6), pp. 686-691.

18. Pant, S., Bressloff, N.W. and Limbert, G., 2012. Geometry Parameterization and Multidisciplinary Constrained Optimization of Coronary Stents. Biomechanics and Modeling in Mechanobiology, 11(1-2), pp. 61-82.

19. Pauck, R. and Reddy, B., 2015. Computational Analysis of the Radial Mechanical Performance of PLLA Coronary Artery Stents. Medical Engineering & Physics, 37(1), pp. 7-12.

20. Schiavone, A. and Zhao, L., 2015. A Study of Balloon Type, System Constraint and Artery Constitutive Model used in Finite Element Simulation of Stent Deployment. Mechanics of Advanced Materials and Modern Processes, 1(1), pp. 1-15.

21. U.S. Food and Drug Administration, Center for Devices and Radiological Health (CDRH). Absorb GT1™ Bioresorbable Vascular Scaffold (BVS) System - P150023, Approval letter, 5 July, 2016. Retrieved 17 March, 2017, from http://www.accessdata.fda.gov/cdrh_docs /pdf15/P150023a.pdf.

22. Witzke, D.R., 1997. Introduction to Properties, Engineering, and Prospects Of Polylactide Polymers.

11. Acknowledgements

The authors wish to acknowledge funding from the Engineering and Physical Sciences Research Council (EPSRC) and the research institutions involved in the Bi-Stretch-4-Biomed collaborative research project (California Institute of Technology, University of Warwick and ENEA: Italian National Agency for New Technologies, Energy and Sustainable Economic Development). The simulations performed in this work were performed on the High Performance Computing (HPC) Windows Cluster at Queen’s University Belfast (QUB).